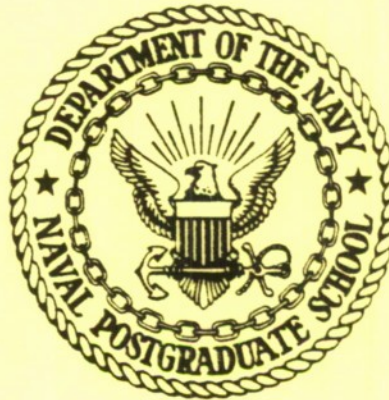


NPS69-79-007PR

NAVAL POSTGRADUATE SCHOOL

Monterey, California



EFFECTS OF CAVITATION ON UNDERWATER
SHOCK LOADING - PLANE PROBLEM, PART I

Robert Eugene
R. E. NEWTON
July 1979

Progress Report for Period April 1979 -
June 1979

TC
171
N521

Approved for Public Release: Distribution Unlimited

Prepared for: Defense Nuclear Agency
Washington, DC 20305

20091105035

TC
171
N521

Naval Postgraduate School
Monterey, California

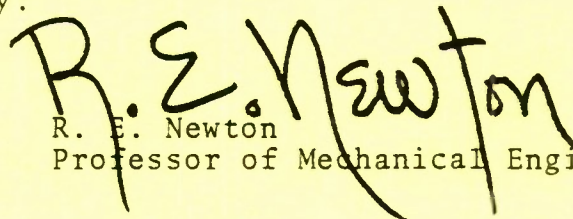
Rear Admiral T. F. Dedman
Superintendent

Jack R. Borsting
Provost

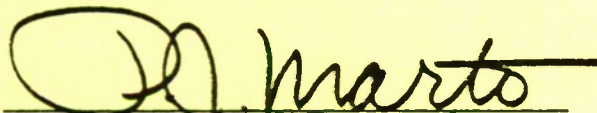
The work reported herein was supported by the Defense Nuclear
Agency SPSS.

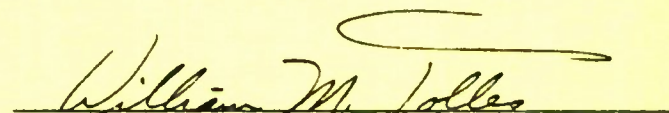
Reproduction of all or part of this report is authorized.

This report was prepared by:


R. E. Newton
Professor of Mechanical Engineering

Reviewed By:


Paul J. Marfo, Chairman
Department of Mechanical
Engineering


W. M. Tolles
Dean of Research

SECURITY CLASSIFICATION OF THIS PAGE (When Data Entered)

REPORT DOCUMENTATION PAGE		READ INSTRUCTIONS BEFORE COMPLETING FORM
1. REPORT NUMBER NPS69-79-007PR	2. GOVT ACCESSION NO.	3. RECIPIENT'S CATALOG NUMBER
4. TITLE (and Subtitle) EFFECTS OF CAVITATION ON UNDERWATER SHOCK LOADING - PLANE PROBLEM, PART 1		5. TYPE OF REPORT & PERIOD COVERED Progress April-June 1979
		6. PERFORMING ORG. REPORT NUMBER NPS69-79-007PR
7. AUTHOR(s) R. E. Newton		8. CONTRACT OR GRANT NUMBER(s) MIPR 79-608
9. PERFORMING ORGANIZATION NAME AND ADDRESS Naval Postgraduate School Monterey, CA 93940		10. PROGRAM ELEMENT, PROJECT, TASK AREA & WORK UNIT NUMBERS Y99QAXSF501 Work Unit 16
11. CONTROLLING OFFICE NAME AND ADDRESS Defense Nuclear Agency SPSS Washington, D. C. 20305		12. REPORT DATE July 1979
		13. NUMBER OF PAGES
14. MONITORING AGENCY NAME & ADDRESS (if different from Controlling Office)		15. SECURITY CLASS. (of this report) UNCLASSIFIED
		15a. DECLASSIFICATION/DOWNGRADING SCHEDULE
16. DISTRIBUTION STATEMENT (of this Report) Approved for Public Release: Distribution Unlimited		
17. DISTRIBUTION STATEMENT (of the abstract entered in Block 20, if different from Report)		
18. SUPPLEMENTARY NOTES		
19. KEY WORDS (Continue on reverse side if necessary and identify by block number) Underwater shock, cavitation, finite elements		
20. ABSTRACT (Continue on reverse side if necessary and identify by block number) Development and testing of a finite element program for shock-induced cavitation is described. A displacement potential function is the dependent variable used. Graphical output is presented for an encounter which induces repeated cavitation.		

EFFECTS OF CAVITATION ON UNDERWATER SHOCK LOADING - PLANE PROBLEM, PART I

1. Introduction

In Ref. 1 possible problem formulations for predicting the effects of cavitation on underwater shock propagation were examined. It was concluded that using either the displacement potential (a scalar) or the particle displacement (a vector) as the dependent variable could produce useful results.

Ref. 2 gave a summary account of an unsuccessful effort to use ADINA for applications with axisymmetric geometry.

The present report is a summary of progress to date in developing a capability for modeling a two-dimensional fluid region in which a structure is submerged. Examination of available codes disclosed no candidate allowing implementation of the displacement potential formulation, with cavitation, for the fluid and simultaneously permitting an appropriately coupled structural model. Accordingly, an ad hoc code for the fluid has been developed. A compatible structural code is being constructed. All codes referred to in this report are written in FORTRAN IV.

2. Program Development

2.1 Mesh Generator (MGNEW)

For a plane problem with a cylindric structure whose length is normal to the plane, the fluid region is the portion of the plane exterior to a circle (radius A). Taking advantage of symmetry and truncating gives the rectangular region of

Fig. 1. The mesh is generated from a set of super-elements as shown in Fig. 2. The transitional super-elements (those adjacent to the structure) each have two curved sides. The remaining elements are square. Note that, if each quadrant of the structural "hole" is treated as an element, the region is topologically equivalent to MU layers, each containing $ML + MR$ squares. In the region of Fig. 2 the entry face is at $x = MR*(0.9*A)$ and the exit face at $x = ML*(0.9*A)$. The top face is at $y = MU*(0.9*A)$.

In the finite element grid each super-element is subdivided $N*N$. The final elements are four-noded quadrilaterals using linear shape functions. For the transitional elements the additional nodes are found by using quadratic isoparametric shape functions for mapping.* The square grid on which the element mesh is based includes $N*(2*N+1)$ nodes which are inside the structure. It is advantageous to retain these nodes in the numbering scheme.

All of the nodal locations within the transition region can be derived from those in the sector from 0° to 45° by successive reflections. It follows that there are only $(3*N+1)*N/2$ distinct transition elements for which fluid "mass" and "stiffness" matrices need to be calculated. The remaining elements are identical squares and only a single additional pair of fluid matrices is required.

A program (MGNEW) has been written to generate this element grid. Required input data are the structure radius A

*Mapping with isoparametric shape functions is described in Ref. 3.

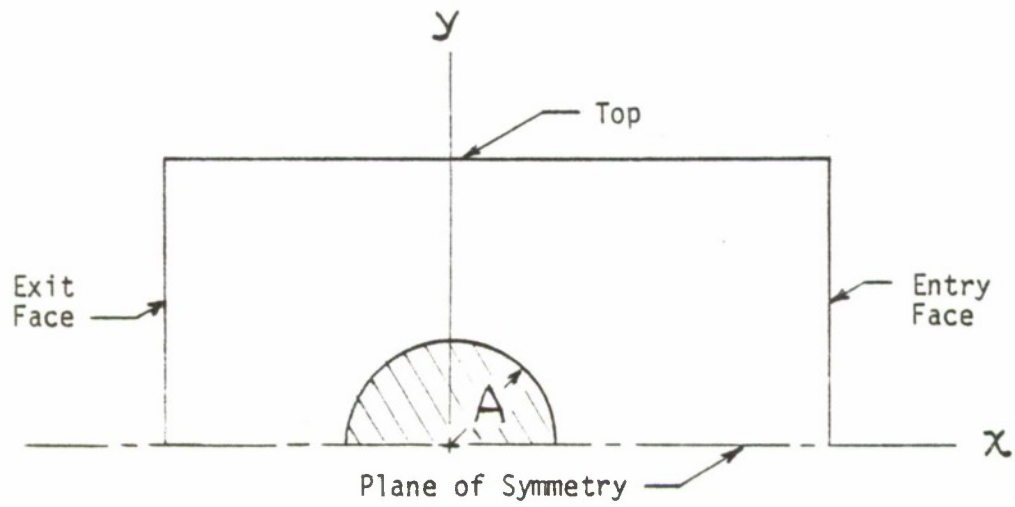


Fig. 1. Fluid region nomenclature

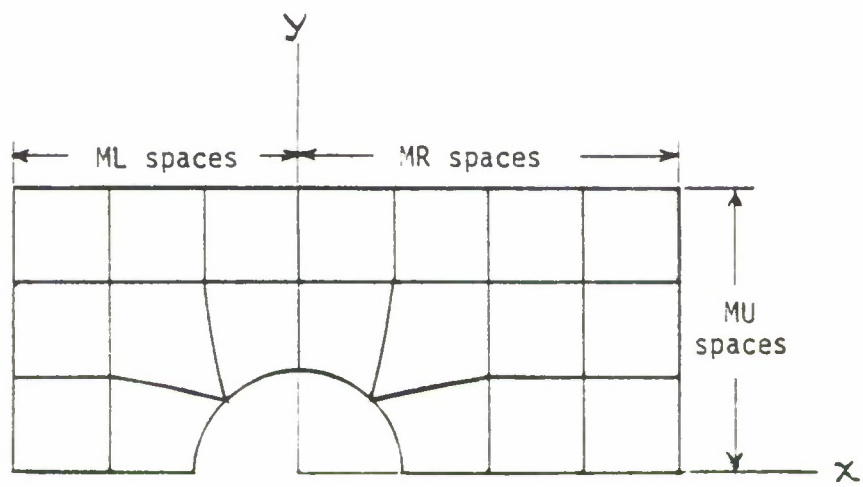


Fig. 2. Super-element grid

and the mesh descriptors ML, MR, MU, and N. Output data include nodal coordinates, numbers of nodes and elements, and global node numbers for each element.

2.2 Fluid Program (DPLPOT)

A program for tracking shock wave propagation, including cavitation, has been developed. Equations for the displacement potential formulation used are given in Ref. 1.

2.21 Initial conditions

A subroutine of the program determines initial values of the displacement potential and its first temporal derivative. These correspond to a uniform hydrostatic pressure plus a plane shock wave with step rise and exponential decay. The shock wave is travelling in the negative x direction with front at $x = A$ at time $t = 0$.

2.22 Boundary conditions

The governing equation requires that values of the normal derivative of the displacement function be specified at boundary nodes. Subroutines are provided to impose a radiation boundary condition on the entry and exit faces. At the entry face explicit provision is made for the continuing entry of the incident shock wave. The analytic basis for these boundary conditions is given in Ref. 1. A radiation boundary condition is also imposed at the top face, again including explicit provision for the passage of the incident shock wave. In the absence of specific intervention the solution scheme enforces a zero value of the normal derivative at boundary points. Accordingly, no boundary inputs are required for the plane of symmetry $y = 0$.

2.23 Temporary structure

Initial testing of the fluid program DPLPOT has been done with a simplified boundary condition at the fluid-structure interface. This condition is that the boundary pressure remains equal to the initial hydrostatic pressure. Physically this corresponds to substituting an inflated cylindric bag for the structure. Such a "hole" in the fluid can readily be made to induce cavitation.

2.24 Coefficient matrices

Coefficient matrices for the fluid are calculated at the element level. The fluid "mass" matrix is lumped (diagonal) rather than consistent. Total storage requirements for element matrices are quite modest because of the limited number of different elements. The diagonal system mass matrix is assembled in a single vector whose length is equal to the number of nodes. No system "stiffness" matrix is assembled.

2.25 Time integration

Numerical integration in time is based on central difference formulas. The calculation is organized in such a way that the nonlinearity introduced by cavitation does not affect the fluid mass or stiffness matrices. Because the integration algorithm is explicit and the mass matrix is diagonal, no matrix decomposition is required. As a result, the central processor time is directly proportional to the number of fluid nodes. Processing time is a linear function of the number of time steps. "Overhead" time requirements for mesh generation, coefficient matrix calculation and establishment of initial values are approximately equivalent

to 9 time steps.

2.3 Fluid Program (VELPOT)

The initial form of the program DPLPOT, described above, required a computationally expensive damping calculation. To avoid this, the alternative of using the velocity potential as the dependent variable was explored. Pertinent equations are given in Ref. 1. For this purpose it was necessary to revise four of the subroutines of DPLPOT. The alternate version, called VELPOT, reduced the central processor time by 35%. Although VELPOT results closely resembled those from DPLPOT, they were not identical. Efforts to account for the discrepancies led to the development of two one-dimensional programs, DIS and VEE, which were made to yield identical results.

Subsequent development of DPLPOT replaced the inefficient damping calculation. This improvement eliminated the computational advantage of VELPOT and VELPOT was abandoned.

2.4 Structural Program (STRUK2)

A structural program has been under development by Jack T. Waller, a thesis student of mine. This program utilizes trigonometric series representations of the loading and displacements of an orthotropic shell in a state of plane strain. It is now being tested separately, but has not yet been coupled with the fluid.

3. Results

Results obtained thus far are relevant to determining when cavitation will occur, how big the cavity will become,

and how long it will persist. For this purpose, various combinations of shock pressure, hydrostatic pressure, and shock decay length have been tested. Effects of region size and shape, element size, length of time step, damping parameter, and total integration time have also been examined.

3.1 Line Printer Plot

The program provides for both tabular and graphical output, but the latter has been the more useful in this phase of the investigation. It is a line printer plot of fluid nodal pressures, repeated at selected time intervals. For the purpose of this plot the nodes of the structural and transition regions are mapped into the topologically equivalent rectangular array.

Fig. 3 shows the arrangement of the line printer plot. The left-hand column is the plane of symmetry (x axis of Fig. 1) and the right-hand column is the "top" face. The entry face is the first row and the exit face is the last row. Along the left-hand edge is a rectangle filled with X's, 4 columns wide and 7 rows high. The X's denote dummy nodes inside the structure. The rows immediately above and below, and the column to the right (all marked H) contain the 17 structural nodes.

The pressure map of Fig. 3 is for hydrostatic pressure 0.2 MPa and shock pressure 2.0 Mpa with a decay length of 15 m. The pressure ranges for the mapping characters are shown at the right. Since the map is for $t = 0$ there are no pressures below hydrostatic.

MESH DATA

A = 5.000 METERS

N = 3 ML = 3 MU = 15 MR = 9 NP = 45

DECAY LENGTH = 15.0 M

ACOUSTIC VELOCITY = 1500. M/S

HYDROSTATIC PRESSURE = 0.2000 MPA

SHOCK PRESSURE = 2.000 MPA

TIME STEP = 0.250 MS

TMAX = 0.0 MS

TMAP = 0.0 MS

ETA = 2.000D-02

PRINT CODE: 121111111 1 112 1

T = 0.0 MS



PRESSURE CODE

Symbol	Pressure range (Mpa)
X	Structure
blank	Cavitated
1	0 - .04
3	.04 - .09
6	.09 - .14
8	.14 - .18
H	.18 - .43
A	.43 - .77
B	.77 - 1.10
C	1.10 - 1.43
D	1.43 - 1.77
E	1.77 - 2.10
F	over 2.10

Fig. 3. Initial pressure map

3.2 Cavitation Example

Fig. 4 exhibits a sequence of pressure maps at 16 ms intervals based on the initial conditions of Fig. 3. Note that the cavity develops rapidly in the first two frames, shrinks in the next two, and is completely closed by 80 ms. The succeeding frames in which the cavity opens again represent the first instance in which this behavior was encountered. It has been established by a longer duration run that the cavity does not open again after 144 ms.



Fig. 4. Cavitation example

REFERENCES

1. Newton, R. E., "Effects of Cavitation on Underwater Shock Loading - Part 1," NPS-69-78-013, Naval Postgraduate School, Monterey, CA, July 1978.
2. Newton, R. E., "Effects of Cavitation on Underwater Shock Loading - Axisymmetric Geometry," NPS-69-78-017PR, Naval Postgraduate School, Monterey, CA, November 1978.
3. Zienkiewicz, O. C., The Finite Element Method, 3rd ed., Chapter 8, McGraw-Hill, London, 1977.

Initial Distribution List

	Copies
1. Research Administration, Code 012A Naval Postgraduate School Monterey, California 93940	1
2. Professor R. E. Newton Mechanical Engineering Department Code 69Ne Naval Postgraduate School Monterey, California 93940	10
3. Weidlinger Associates Consulting Engineers 110 East 59th Street New York, NY 10022 ATTN: Melvin Baron	1
4. Lockheed Missiles and Space Company, Inc. 3251 Hanover Street Palo Alto, California 94304 ATTN: Tom Geers D/52-33 Building 205	1
5. Director Defense Nuclear Agency Washington, D. C. 20305 ATTN: SPSS	10
6. Superintendent Naval Postgraduate School Monterey, California 93940 ATTN: Code 2124 Tech. Rpts. Lib.	2